



## Control of cell motility by interaction of gangliosides, tetraspanins, and epidermal growth factor receptor in A431 versus KB epidermoid tumor cells

Seung-Yeol Park<sup>a,b,c,†</sup>, Seon-Joo Yoon<sup>a,b,†,‡</sup>, Leonardo Freire-de-Lima<sup>a,b</sup>, Jung-Hoe Kim<sup>c</sup>, Sen-itiroh Hakomori<sup>a,b,\*</sup>

<sup>a</sup> Division of Biomembrane Research, Pacific Northwest Research Institute, 720 Broadway, Seattle, WA 98122-4302, USA

<sup>b</sup> Departments of Pathobiology and Global Health, University of Washington, Seattle, WA 98195, USA

<sup>c</sup> Department of Biological Sciences, Korea Advanced Institute of Science and Technology, 373-1, Guseong-dong, Yuseong-gu, Daejeon 305-701, Republic of Korea

### ARTICLE INFO

#### Article history:

Received 5 March 2009

Received in revised form 20 April 2009

Accepted 30 April 2009

Available online 13 May 2009

Dedicated to Professor Hans Kamerling on the occasion of his retirement from Utrecht University, The Netherlands

#### Keywords:

Cell growth

Cell motility

Tyrosine phosphorylation

EtDO-P4

Cell proliferation

Tetraspanins

### ABSTRACT

Growth of epidermoid carcinoma cell lines, A431 and KB, has been known to be controlled by the interaction of epidermal growth factor (EGF) and its receptor (EGFR) with tyrosine kinase. Ganglioside GM3 was previously found to interact with EGFR and to inhibit EGFR tyrosine kinase. However, motility of these cells, controlled by EGFR and ganglioside, was not studied. The present study is focused on the control mechanism of the motility of these cells through interaction of ganglioside, tetraspanin (TSP), and EGFR. Key results are as follows: (i) The level of EGFR expressed in A431 cells is ~6 times higher than that expressed in KB cells, and motility of A431 cells is also much higher than that of KB cells, yet growth of A431 cells is either not affected or is inhibited by EGF. In contrast, growth of KB cells is enhanced by EGF. (ii) Levels of TSPs (CD9, CD82, and CD81) expressed in A431 cells are much higher than those expressed in KB cells, and TSPs expressed in A431 cells are reduced by treatment of cells with EtDO-P4, which inhibits the synthesis of glycosphingolipids (GSLs) and gangliosides. (iii) These TSPs are co-immunoprecipitated with EGFR in both A431 and KB cells, indicating that TSPs are closely associated with EGFR. (iv) High motility of A431 cells is greatly reduced, while low motility of KB cells is not affected, by treatment of cells with EtDO-P4. These results, taken together, suggest that there is a close correlation between high motility of A431 cells and high expression of EGFR and TSPs, and between ganglioside GM3/GM2 and TSP. A similar correlation was suggested between the low motility of KB cells and low levels of EGFR and TSP. The correlation between high motility and high level of EGFR with the ganglioside–TSP complex in A431 cells is unique. This is in contrast to our previous studies that indicate that motility of many types of tumor cells is inhibited by a high level of CD9 or CD82, together with growth factor receptors and integrins.

© 2009 Published by Elsevier Ltd.

### 1. Introduction

Human epidermoid carcinoma cell lines A431 and KB are characterized by a clear expression of epidermal growth factor receptor (EGFR) tyrosine kinase activity.<sup>1–3</sup> Both A431 and KB cells stimulated with epidermal growth factor (EGF) display enhanced tyro-

sine kinase activity, which is inhibited by ganglioside GM3 but not by ganglioside GM1 or sialyl-nLc4.<sup>4</sup> Such an inhibitory effect by ganglioside GM3 was found to be due to the interaction of GM3 ganglioside with the extracellular EGFR domain.<sup>5</sup> Recent studies on the mechanism of such interaction in A431 cells indicated that GM3 interacts with N-linked glycan having multiple GlcNAc termini, expressed in EGFR, and such interaction was assumed to inhibit EGF-induced EGFR tyrosine kinase.<sup>6</sup>

Previous studies on A431<sup>7</sup> and KB cells<sup>8</sup> were focused on cell growth based on EGF-stimulated EGFR tyrosine kinase, and the effect of gangliosides on cell growth through modulation of EGFR kinase activity. No studies have been conducted so far on the regulation of EGFR-dependent cell motility. The present study is based on our recent, incidental observation that A431 cells express much higher levels of TSPs CD9, CD81, and CD82 than do KB cells. These TSPs were shown to interact with ganglioside GM3 or GM2,<sup>9,10</sup> and such ganglioside–TSP complexes were found to inhibit

**Abbreviations:** DMEM, Dulbecco's Modified Eagle's Medium; EtDO-P4, *n*-*theo*-1-(3',4'-ethylenedioxy)phenyl-2-palmitoylamino-3-pyrrolidino-1-propanol; EGFR, epidermal growth factor receptor; FCS, fetal calf serum; FITC, fluorescein isothiocyanate; GM3, NeuAc $\alpha$ 3Gal $\beta$ 4Glc $\beta$ 1Cer; GM2, GalNAc $\beta$ 4[NeuAc $\alpha$ 3]Gal $\beta$ 4Glc $\beta$ 1Cer; GSL, glycosphingolipid; HRP, horseradish peroxidase; ITS, insulin–transferrin–selenium medium; TLC, thin-layer chromatography; T-TBS, TBS (140 mM NaCl–10 mM Tris–HCl, pH 8.0) with addition of 0.05% Tween 20.

\* Corresponding author. Tel.: +1 206 726 1222; fax: +1 206 726 1212.

E-mail address: [hakomori@u.washington.edu](mailto:hakomori@u.washington.edu) (S. Hakomori).

† These authors contributed equally to this study.

‡ Present address: Cardiovascular Biology Research Program, Oklahoma Medical Research Foundation, Oklahoma City, OK 73104, USA.

motility, in addition to growth, of various tumor cells, possibly through integrin-dependent pathways,<sup>9–12</sup> although the exact mechanism still remains unclear. In the present study, we therefore explore how the level of TSPs is correlated with motility of A431 versus KB cells, in association with the level of EGFR expressed in A431 versus KB cells. A novel GSL–TSP–EGFR association in A431 cells, which mediates high cell motility, is clearly demonstrated.

## 2. Materials and methods

### 2.1. Cell lines

Two types of human epidermoid carcinoma cell lines, A431 and KB, were purchased from ATCC and were originally described in Refs. 7 and 8, respectively. These cells were grown and maintained in DMEM supplemented with 10% FCS, 100 IU/mL penicillin, and 100 unit/mL streptomycin at 37 °C in 5% CO<sub>2</sub>–95% air.

### 2.2. Antibodies and other materials

Antibodies used were as follows: mouse anti-GM2 IgM mAb MK1-8<sup>13</sup> was donated by Reiji Kannagi (Aichi Cancer Center, Nagoya). Mouse anti-GM3 IgG3 mAb DH2 was established in this laboratory.<sup>14</sup> Mouse anti-EGFR mAb, rabbit polyclonal anti-CD9 IgG, rabbit polyclonal anti-CD82 IgG, mouse monoclonal anti-integrin  $\alpha$ 3 IgG<sub>1</sub>, goat anti-mouse IgG–HRP, goat anti-rabbit IgG–HRP, and bovine anti-goat IgG–HRP (all obtained from Santa Cruz Biotechnology, Santa Cruz, CA); mAb anti-phospho-Tyr (PY20, BD Biosciences); mouse anti-CD81 mouse IgG2a (Beckman–Coulter, Brea, CA); and mouse anti- $\gamma$ -tubulin mAb (Sigma, St. Louis, MO). PVDF membrane was obtained from Millipore Corp. (Billerica, MA). A cell proliferation assay kit including WST-1–ECS solution was obtained from Chemicon (Temecula, CA). Lipid stain reagent, Primulin, was obtained from Sigma–Aldrich Chemical Co. (Milwaukee, WI). EtDO-P4, the potent inhibitor of GlcCer synthase,<sup>15</sup> was donated by James A. Shayman (Dept. of Internal Medicine, Univ. of Michigan).

### 2.3. Expression pattern of epidermal growth factor receptor in A431 and KB cells

Levels of epidermal growth factor receptor (EGFR) expressed in A431 and KB cells were determined by Western blot analysis, followed by densitometry of the EGFR band by the SCION IMAGE program, relative to  $\gamma$ -tubulin as the loading control, which was blotted in a separate membrane.

Cells ( $7 \times 10^5$ ) were grown in a 100-mm round culture plate until 80% confluency. Cultured cells, harvested by a rubber scraper, were lysed in RIPA buffer (1% Triton X-100, 0.1% SDS, 0.5% sodium deoxycholate, 5 mM tetrasodium pyrophosphate, 50 mM sodium fluoride, 1 mM Na<sub>3</sub>VO<sub>4</sub>, 5 mM EDTA, 150 mM NaCl, 20 mM Tris–HCl, pH 7.5, 2 mM phenylmethanesulfonyl fluoride, and 0.076 IU/mL aprotinin), and centrifuged at 13,000 rpm for 10 min. A defined amount of the lysate protein (20  $\mu$ g) determined by the Micro BCA™ Protein Assay Kit, was subjected to SDS–PAGE, followed by transfer to PVDF membrane. After blocking with 5% skim milk for 2 h, the membrane was rinsed with T–TBS, and bands for EGFR and  $\gamma$ -tubulin in each separate membrane were blotted with respective mAbs overnight at 4 °C. Membranes were rinsed, incubated with goat anti-mouse IgG–HRP, and developed by the Super-signal Chemiluminescence Substrate Kit (Pierce).

### 2.4. Determination of A431 and KB cell growth with or without various concentrations of EGF

The effect of EGF on cell growth was studied by dose-dependent and time-dependent changes of EGF (i) an increase in cell number

determined under a microscope; (ii) <sup>3</sup>H-thymidine incorporation as described below.

A431 or KB cells ( $2 \times 10^4$ ) in 400  $\mu$ L of 10% FCS–DMEM were plated in 24-well plates, incubated in a CO<sub>2</sub> incubator at 37 °C for 24 h, washed twice with 5% FCS–DMEM, and further cultured in 200  $\mu$ L of 5% FCS–DMEM, without addition of EGF (0 pM), or with addition of various concentrations of EGF (1.7 pM, 3.4 pM, or 3.4 nM) for various durations (1, 3, or 5 days). Fresh 5% FCS–DMEM containing EGF was changed every 24 h. At the indicated time, the wells were washed three times with 0.5 mL of 5% FCS–DMEM and subjected to two procedures: (i) Cells were stained with Trypan Blue, and cell numbers were counted in all nine sections of the hemocytometer under a microscope. (ii) Cells were further cultured in 200  $\mu$ L 5% FCS–DMEM containing <sup>3</sup>H-thymidine (10  $\mu$ Ci/mL) in a 37 °C CO<sub>2</sub> incubator for 2 h, detached by treatment with 200  $\mu$ L of trypsin–EDTA, and transferred into a scintillation counting vial. After recovering all cells by washing with  $5 \times 0.5$  mL of PBS, <sup>3</sup>H was counted.

### 2.5. Colorimetric determination of EGF-induced cell proliferation

Cell proliferation, based on activity of mitochondrial dehydrogenases, was colorimetrically determined using Chemicon's WST-1 reagent, according to the manufacturer's instructions. Briefly, A431 or KB cells ( $1 \times 10^5$ ) suspended in 100  $\mu$ L culture medium (serum-free DMEM, F12–DMEM + insulin–transferrin–selenium medium [ITS], and 5% FCS–DMEM) were plated into each well of a 96-well plate, incubated for 24 h, and washed twice with 100  $\mu$ L of each medium. The cells were further incubated in 100  $\mu$ L of each culture medium containing EGF (0, 1.7 pM, 3.3 pM, 6.6 pM, 13.3 pM, 26.6 pM, 53.1 pM, 106 pM, 213 pM, 425 pM, 850 pM, 1.7 nM, 3.4 nM, 6.8 nM, and 13.6 nM). After incubation for 44 h, 10  $\mu$ L WST-1–ECS solution from the Cell Proliferation Assay Kit was added to each well, cells were incubated for 3 h, shaken thoroughly for 1 min on a shaker, and the absorbance was measured using a microplate reader ( $\gamma$ 1 = 405 nm,  $\gamma$ 1 = 630 nm). This assay is based on reductive cleavage of the tetrazolium salt WST-1 to formazan by cellular mitochondrial dehydrogenases.

### 2.6. Flow cytometric analysis of expression of gangliosides GM3 and GM2, and tetraspanins in A431 and KB cells

Cells were cultured in a T-75 flask containing DMEM with 10% FCS until 80% confluency, detached by 2 mL of 1 mM EDTA–PBS, added to 2 mL of 10% FCS–DMEM, and centrifuged at 1000 rpm for 5 min. After counting the cell number, cells ( $1 \times 10^5$ ) were placed in a 1.5-mL Eppendorf tube, centrifuged at 1000 rpm for 5 min, washed with 1% BSA–PBS, and incubated with (i) 100  $\mu$ L of mouse IgG (10  $\mu$ g/mL in 1% BSA–1% goat serum–0.05% azide), (ii) mouse IgM (10  $\mu$ g/mL in 1% BSA–1% goat serum–0.05% azide), (iii) anti-GM3 DH2, and (iv) anti-GM2 MK1-8, on ice for 1.5 h. After washing twice with 0.5 mL of 1% BSA–PBS, the cells were mixed with 50  $\mu$ L of goat anti-mouse Ig (G+M)–FITC (25  $\mu$ g/mL) and incubated on ice for 45 min in the dark. After centrifugation and washing twice with 0.5 mL of PBS, cells were fixed with 100  $\mu$ L of 1% paraformaldehyde–PBS overnight. Stained cells were subjected to flow cytometric analysis.

### 2.7. Effect of inhibition of the GSL synthesis by EtDO-P4 on the phosphorylation of EGFR

To explore the functional role of GM3, GM2, and other GSLs on the growth and motility of A431 and KB cells, EtDO-P4, the potent inhibitor of GlcCer synthase, was used. This treatment inhibits the synthesis of all GSLs derived from GlcCer, without significant

enhancement of ceramide level.<sup>11,15,16</sup> A431 and KB cells ( $7 \times 10^5$ ) were plated in a 100-mm round culture plate for 24 h. After cells were attached to the plate, they were rinsed with 10% FCS–DMEM and cultured in 10% FCS–DMEM with added 1  $\mu$ M EtDO–P4 for 72 h. After rinsing with serum-free DMEM, cells were cultured in serum-free DMEM with or without addition of 1  $\mu$ M EtDO–P4 for 24 h. For stimulation of EGFR, cells were rinsed with serum-free DMEM, and grown in serum-free DMEM with addition of 100 ng/mL EGF for 1 h. GSLs extracted from cells were subjected to TLC or immunostaining as described below. For determination of integrin and tetraspanin, the cell lysate prepared in RIPA buffer was subjected to Western blotting using various antibodies as described below.

## 2.8. GSL extraction, thin-layer chromatography (TLC), and immunostaining

GSLs expressed in A431 and KB cells treated with or without EtDO–P4 were determined as below. Cells pre-treated with or without 1  $\mu$ M EtDO–P4 were grown in a 150-mm round culture plate containing 10% FCS–DMEM as described above, and harvested in a 50-mL glass tube containing 1 mL of 2:1 chloroform–methanol (C–M). After sonication, the cell pellet was mixed with 1 mL of 55:25:20 2-propanol–hexane–water, sonicated, and centrifuged.<sup>17</sup> The supernatant was combined with 2:1 C–M extract, and dried under an  $N_2$  stream. The dried residue was subjected to isolation of the GSL fraction by alkaline hydrolysis of phospholipids as described previously.<sup>18</sup> Briefly, the residue was dissolved in 2 mL of 0.1 M NaOH–methanol and incubated for 2 h at 40 °C. After neutralization using 200  $\mu$ L of 1 N HCl, the released fatty acids were eliminated by mixing with 2 mL of hexane and shaking. After standing at room temperature, the supernatant was aspirated, and the lower layer was evaporated under an  $N_2$  stream. The residue was dissolved in 1 mL of 6:4 methanol–water (M–W), and applied onto a SepPak C<sub>18</sub> cartridge (Varian, Palo Alto, CA) that had been prewashed with 2:1 C–M (3 mL  $\times$  4) and 6:4 M–W. After rinsing five times with 1 mL of 6:4 M–W, the C<sub>18</sub> cartridge-bound fraction was eluted twice with 1 mL of 2:1 C–M, evaporated under an  $N_2$  stream, and dissolved in 50  $\mu$ L of 2:1:0.1 chloroform–methanol–water (C–M–W).

To determine the GSL pattern, 4  $\mu$ L GSL was spotted on a TLC plate and subjected to TLC in 65:20:8 or 60:25:8 C–M–W for less polar GSLs such as GM3, GM2, and GM1; and in 5:4:1 C–M–W with 0.2% CaCl<sub>2</sub> for highly polar GSLs (GSLs with >5 sugars and >2 sialic acids). After air drying, the TLC plates were stained by spraying 0.01% Primulin for detection of all types of lipids,<sup>19</sup> followed by staining with 2% orcinol in 2 M H<sub>2</sub>SO<sub>4</sub> for detection of all types of glycosyl residues.

Immunostaining for detection of GM2 and GM3 was performed as follows. A TLC plate was blocked with blocking solution (1% BSA–PBS) in T–TBS [TBS (140 mM NaCl, 10 mM Tris–HCl, pH 8.0)–0.05% Tween 20] for 1 h at room temperature. After rinsing five times with T–TBS, plates were incubated with anti-GM2 antibody (1:1000 diluted in blocking solution) or with anti-GM3 antibody (cell culture supernatant) overnight at 4 °C. After rinsing five times with T–TBS, plates were incubated with anti-mouse IgM–HRP (1:1000 diluted in blocking solution) against anti-GM2 mAb and with anti-mouse IgG–HRP (1:1000 diluted in blocking solution) against anti-GM3 mAb for 1 h at room temperature. Plates were developed by the Supersignal West Pico Chemiluminescence Substrate Kit (Pierce, Rockford, IL).<sup>20</sup>

## 2.9. SDS–PAGE and Western blot

Cell lysate prepared in RIPA buffer as described above was subjected to SDS–PAGE (12.5% acrylamide) and transferred onto a

PVDF membrane. After blocking with 5% skim milk for 2 h, followed by rinsing with T–TBS, the membrane was incubated separately with various antibodies as described in Section 2.2. After rinsing five times with T–TBS for 5 min, the membrane was incubated with a secondary antibody as described in Section 2.2. After rinsing with T–TBS, the membrane was developed by the Supersignal Chemiluminescence Substrate Kit (Pierce).

## 2.10. Cell motility determination in A431 and KB cells

Cell motility was determined by a phagokinetic assay on a gold sol-coated plate.<sup>21</sup> Briefly, a 24-well plate was coated with 1% BSA for 3 h, washed with ethanol, and sterilized under UV light for 30 min. Colloidal gold was prepared as follows: 16.4 mL of distilled water and 0.6 mL of 365 mM Na<sub>2</sub>CO<sub>3</sub> were boiled and mixed with 1.8 mL of 14.5 mM AuHCl<sub>4</sub> and 1.8 mL of 0.1% formaldehyde. After drying and coating with colloidal gold for 40 min, A431 and KB cells ( $5 \times 10^2$ ) treated with or without EtDO–P4 for 72 h were cultured in a 24-well plate containing 10% FCS–DMEM with or without EtDO–P4 for 18 h. The gold sol-coated area cleared by each cell was measured by the IMAGEJ program, for  $\geq 30$  cells of A431 and KB, respectively. Measurements were repeated four times.

## 2.11. Co-immunoprecipitation procedure

### 2.11.1. Fractions used for co-IP

The PNF (post-nuclear fraction) was prepared as described previously.<sup>12</sup> A431 and KB cells ( $2 \times 10^6$ ) were grown in 100-mm round culture plates until confluency. Cells harvested by a rubber scraper were lysed in 1% Brij 98 lysis buffer (1% Brij 98, 25 mM

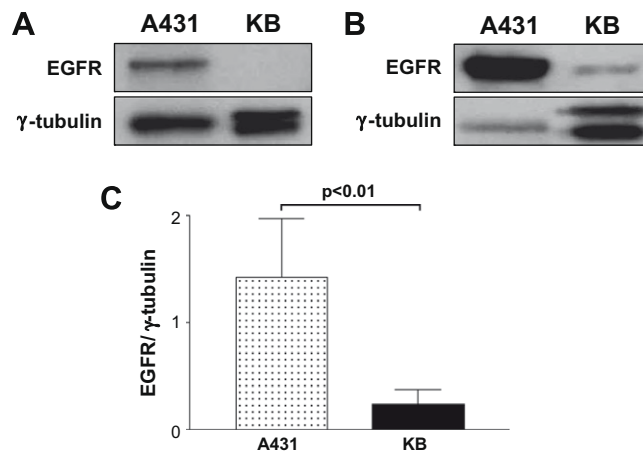


**Figure 1.** EGFR of A431 and KB cells. Cells ( $7 \times 10^5$ ) grown in a 100-mm round plate were harvested and lysed in RIPA buffer. A defined amount (equivalent to 20  $\mu$ g protein) of cell lysate was subjected to SDS–PAGE under reducing condition, followed by Western blot analysis as described in Section 2.3. The EGFR band (~170 kDa molecular mass) was blotted by anti-EGFR mAb directed to the cytoplasmic domain of EGFR, and  $\gamma$ -tubulin (55 kDa) in a separate membrane was detected by anti- $\gamma$ -tubulin antibody. The relative intensity of the EGFR band from A431 versus KB cells was determined by densitometry with SCION IMAGE program. The difference between A431 and KB cells based on triplicate analysis was highly significant ( $P$  value < 0.01). Panel A: The EGFR band from A431 cells was clearly observed, but no clear band was observed from KB cells, when comparable levels of  $\gamma$ -tubulin from both cells were blotted. Panel B: In order to observe a clear EGFR band from KB cells, a much larger quantity of lysate was required to be blotted. This panel shows an example in which at least a sixfold higher quantity of the  $\gamma$ -tubulin band for KB cells than that for A431 cells was required. Panel C: The relative intensity of EGFR expressed in A431 versus KB cells based on results shown in Panel B. Experiments were repeated thrice; mean  $\pm$  SD and  $P$ -values are presented. Lane 1, A431 cells; lane 2, KB cells. Standard deviation of EGFR blot per  $\gamma$ -tubulin blot is shown for each column, and the significance of the difference between A431 and KB cells:  $P$  < 0.01.

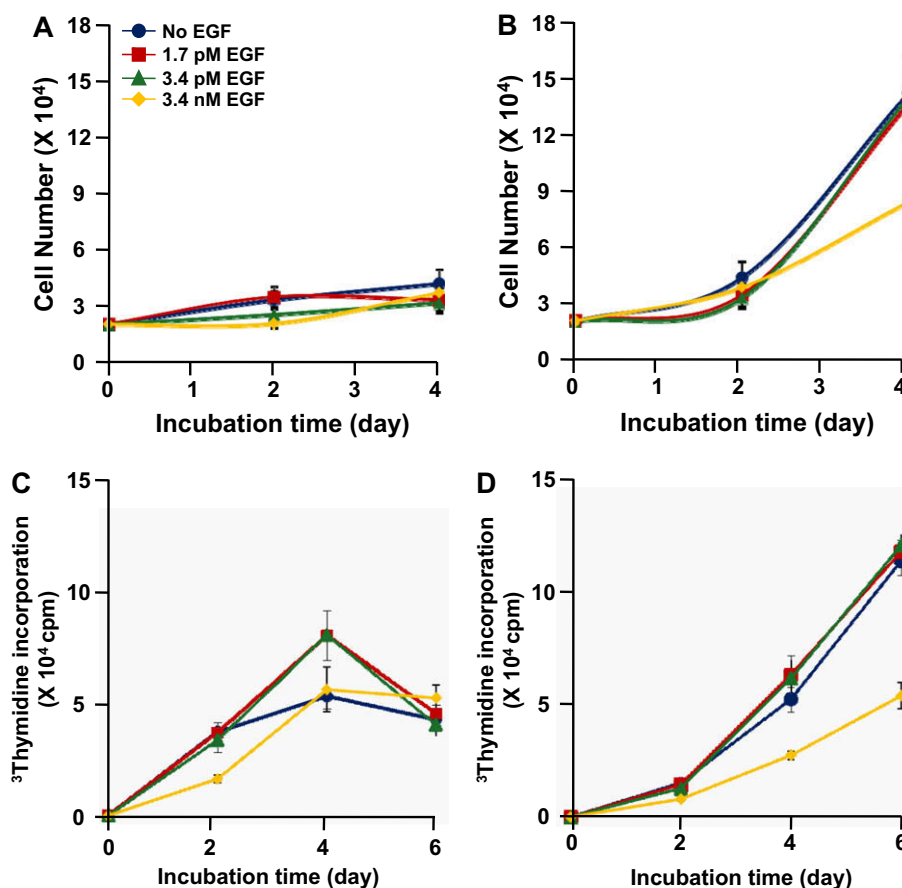


**Figure 2.** The effect of EGF on cell growth in A431 and KB cells. Panels A and B: The effect of EGF on the increase in cell numbers, as determined under a microscope. Cells ( $2 \times 10^4$ ) cultured in a 24-well plate containing 5% FCS–DMEM for 24 h were further cultured in the same medium containing various concentrations of EGF (no EGF, 1.7 pM, 3.4 pM, and 3.4 nM) as indicated by different colors (see below). Cell number was counted on a hemocytometer under a microscope, and nine sites were counted and calculated. Time of growth (days) is shown on the abscissa. Cell number is shown on the ordinate. Panels C and D:  $^3\text{H}$ -thymidine incorporation was measured by a scintillation counter after further culturing the cells in same medium containing  $^3\text{H}$ -thymidine (10  $\mu\text{Ci}/\text{mL}$ ) in a  $37^\circ\text{C}$   $\text{CO}_2$  incubator for 2 h. Experiments were repeated thrice; mean  $\pm$  SD are presented. Circle  $\bullet$ – $\bullet$ , no EGF. Square  $\blacksquare$ – $\blacksquare$ , 1.7 pM EGF. Triangle  $\blacktriangle$ – $\blacktriangle$ , 3.4 pM EGF. Rhombus  $\blacklozenge$ – $\blacklozenge$ , 3.4 nM EGF.

HEPES buffer, pH 7.5, 150 mM NaCl, and 5 mM EDTA) containing 75 units aprotinin and 2 mM phenylmethanesulfonyl fluoride. The suspension was left on ice for 30 min and lysed with 25G syringe 15 times on ice. After centrifugation at 2500 rpm for 5 min at

$4^\circ\text{C}$ , the supernatant (post-nuclear fraction) was quantified by a Micro BCA<sup>TM</sup> protein assay kit based on a standard curve using commercial BSA, and then subjected to 12.5% SDS–PAGE and Western blot analysis.

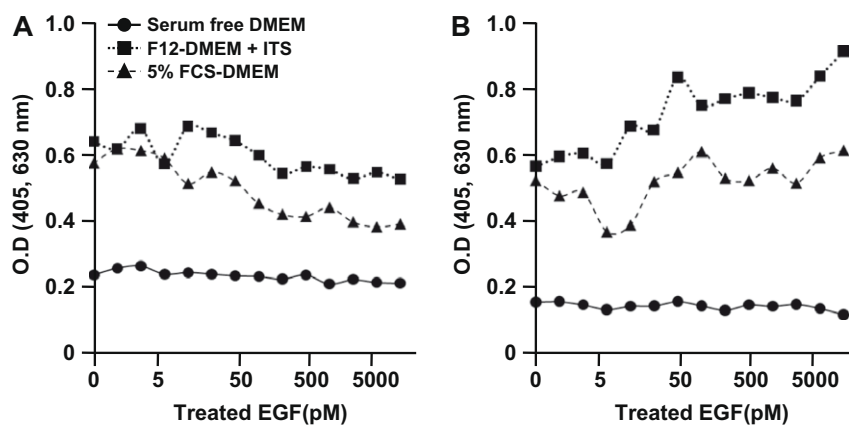


**Figure 3.** The effect of EGF on cell proliferation in A431 and KB cells determined by colorimetric analysis. A431 or KB cells ( $1 \times 10^5$ ) plated in a 96-well plate were cultured in serum-free DMEM, or F12–DMEM + ITS, or 5% FCS–DMEM for 24 h. Various concentrations of EGF were then added to the medium, and culturing was continued for 44 h. Next, WST-1/ECS solution from Cell Proliferation Assay Kit was added to medium, and culturing was continued for 3 h in a  $\text{CO}_2$  incubator at  $37^\circ\text{C}$ . Cell proliferation with various concentrations of EGF (pM) as indicated on the abscissa was measured as absorbance ( $\gamma_1 = 405 \text{ nm}$ ,  $\gamma_2 = 630 \text{ nm}$ ) as indicated on the ordinate. Each data point shown represents mean value from three experiments. Panel A, A431 cells; Panel B, KB cells. Circle  $\bullet$ – $\bullet$ , serum-free DMEM. Square  $\blacksquare$ – $\blacksquare$ , F12–DMEM + ITS. Triangle  $\blacktriangle$ – $\blacktriangle$ , 5% FCS–DMEM.



### 2.11.2. Determination of interaction between EGFR and tetraspanin by co-IP

To determine the interaction between EGFR and TSP, we performed co-IP. Briefly, the post-nuclear fraction (400 µg protein/400 µL) was mixed with protein A–G-agarose beads (~40 µL bead volume), rotated for 3 h at 4 °C, and centrifuged at 2500 rpm for 5 min at 4 °C (i.e., pre-clearing). The supernatant was supplemented with 3 µg of anti-EGFR antibody, and the mixture was rotated overnight at 4 °C. The protein A–G-agarose beads were added to the mixture, rotated for 3 h at 4 °C, and centrifuged at 2500 rpm for 5 min at 4 °C. After washing twice with 1 mL of lysis buffer, the immunoprecipitates were mixed with SDS–PAGE sample buffer and subjected to SDS–PAGE and Western blot analysis with antibodies directed to TSPs, as described above.

## 3. Results

### 3.1. Level of EGFR expressed in A431 versus KB cells

Expression levels of EGFR in A431 versus KB cells were determined by Western blot analysis. The EGFR blot from A431 cells was clearly observed, but that from KB cells was not observed when similar levels of  $\gamma$ -tubulin were compared (Fig. 1A). In order to observe the EGFR blot from KB cells, at least a sixfold higher level of total protein from KB cells than that from A431 cells was required for comparison; that is, a KB cell extract with ~6 times higher  $\gamma$ -tubulin level was required. Under these conditions, the EGFR blot from KB cells was observable (Fig. 1B). The relative abundance of the EGFR band expressed in A431 versus KB cells, using sufficient cell extract to get a clear band for both A431 and KB cells, from triplicate experiments, is shown in Figure 1C.

### 3.2. Difference of growth in A431 versus KB cells

The increase in cell numbers for A431 and KB cells in DMEM with 5% FCS, in the absence or presence of various concentrations of EGF, was studied as described in Section 2.4. The increase in cell numbers of A431 cells was minimal during 4 days with or without addition of EGF. The increase in cell numbers was essentially unchanged with addition of 3.4 pM or 3.4 nM EGF (Fig. 2A). In contrast, an increase in cell number of KB cells between 2 and 4 days was clearly observed with or without EGF addition (0 pM, 1.7 pM, and 3.4 pM). A slightly lower increase was observed with addition of 3.4 nM EGF (Fig. 2B).

The effect of EGF on DNA synthesis was studied by  $^3\text{H}$ -thymidine incorporation. A431 cells showed higher thymidine incorporation at early stage of culture, days 2–4 (with or without EGF addition), but it declined significantly at 4–6 days with 3.4 pM or 3.4 nM EGF (Fig. 2C). In contrast, KB cells showed lower thymidine incorporation response at early stages of culture, but displayed clearly higher incorporation than A431 cells at 3–5 days after EGF addition (days 4–6 of culture) (Fig. 2D).

### 3.3. Effect of EGF on proliferation of A431 and KB cells

The proliferation pattern of A431 and KB cells in response to increasing EGF addition was studied in a few different culture media as described in Section 2.5. Growth of A431 cells in both serum-free F12–DMEM + ITS medium and 5% FCS–DMEM was down-regulated when EGF concentration was >50 pM (Fig. 3A). In contrast, growth of KB cells in the same media was clearly enhanced when the EGF concentration was >50 pM (Fig. 3B). Neither A431 cells nor KB cells displayed EGF-induced proliferation in serum-free DMEM without addition of ITS medium.

### 3.4. Expression pattern of GM3 and GM2 in A431 and KB cells by flow cytometry

The expression patterns of GM3 and GM2 in A431 and KB cells were studied by flow cytometric analysis using goat anti-mouse Ig (G+M)–FITC, as described in Section 2.6. Surface reactivity of A431 cells with anti-GM3 mAb was higher than that of KB cells (Fig. 4, panel A vs panel B), whereas reactivity of KB cells with anti-GM2 mAb was slightly higher than that of A431 cells (panel C vs panel D). These flow cytometric data were based on the same cell number ( $1 \times 10^5$ ). Relative expression of these gangliosides at the cell surface is more reliable than a TLC pattern with orcinol–sulfuric acid or immunostaining.

### 3.5. GM3 and GM2 in A431 and KB cells determined by thin-layer chromatography with antibody staining

To determine the pattern of GSLs from A431 and KB cells, we performed TLC, which was stained first by Primulin spray<sup>19</sup> (Fig. 5A–a, left panel), and then by orcinol–sulfuric acid (Fig. 5A–b, right panel). Bands corresponding to GM3 or GM2 from A431 and KB cells (lanes 4 and 6, respectively) were reduced or depleted in EtDO–P4-treated cells (lanes 5 and 7). Presence of GM2 and GM3 in A431 and KB cells was confirmed by TLC immunostaining using anti-GM2 mAb MK1-8 (Fig. 5B–a) or anti-GM3 mAb DH2 (Fig. 5B–b). While the GM2 level was similar between A431 and KB cells, the GM3 level was lower in A431 cells than in KB cells. The level of GM3 in both A431 and KB cells was lower than that of GM2.

### 3.6. Effect of EtDO–P4 on expression of EGFR and tetraspanin in A431 and KB cells

Expression patterns of EGFR, its tyrosine phosphorylation, integrins, and TSPs were studied in A431 and KB cells cultured with or without EtDO–P4 pre-treatment. The EGFR band was slightly reduced by EtDO–PH–P4 treatment (Fig. 6A, row1; Fig. 6B–a, column

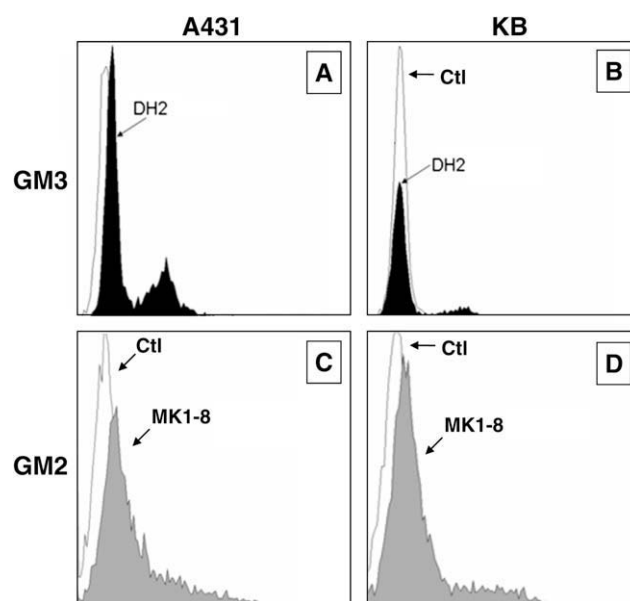


**Figure 4.** Flow cytometric analysis of GM3 and GM2 expressed in A431 and KB cells. Cells ( $1 \times 10^5$ ) were washed with 1% BSA–PBS, incubated with (i) mouse IgG (as control) or anti-GM3 IgG3 mAb DH2; (ii) mouse IgM (as control) or anti-GM2 IgM mAb MK1-8, on ice for 1.5 h, washed, mixed with Alexa Fluor 488 goat anti-mouse IgG (H+L) (for case i) or goat anti-mouse Ig (G+M)–FITC (for case ii), kept on ice for 45 min, washed, fixed with 1% paraformaldehyde, and subjected to flow cytometric analysis as described in Section 2.6. Panels A and C: A431 cells. Panels B and D: KB cells.

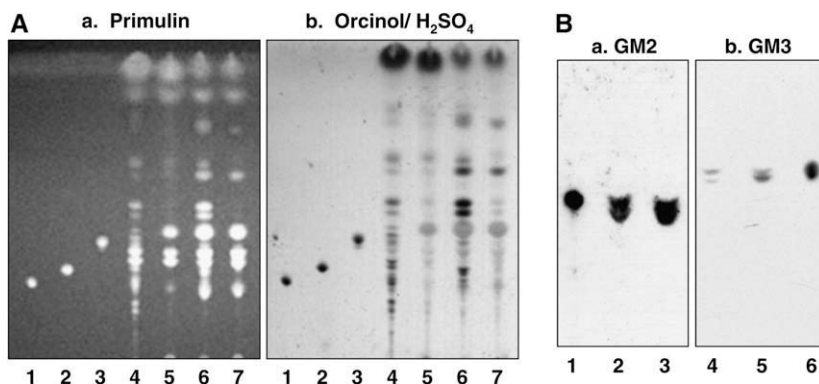


**Figure 5.** TLC and immunostaining of GSLs from A431 and KB cells. Panel A: GSLs extracted from A431 and KB cells cultured with or without EtDO-P4 were subjected to TLC and stained with Primulin (A-a) or orcinol–sulfuric acid (A-b). Lane 1: GM1; lane 2: GM2; lane 3: GM3; lane 4: GSLs from A431 cells cultured without EtDO-P4; lane 5: GSLs from A431 cells cultured with EtDO-P4; lane 6: GSLs from KB cells cultured without EtDO-P4; and lane 7: GSLs from KB cells cultured with EtDO-P4. Panel B: GSLs from A431 and KB cells were subjected to immunostaining using anti-GM2 mAb MK1-8 (B-a), and anti-GM3 mAb DH2 (B-b) mAbs. Lane 1: standard GM2; lanes 2 and 4: GSLs from A431 cells; lanes 3 and 5: GSLs from KB cells; and lane 6: standard GM3.

1 vs column 2). Tyrosine phosphorylation associated with EGFR (P-EGFR) was not affected by EtDO-P4 treatment in either A431 or KB cells (Fig. 6A, row 2; Fig. 6B-b, column 1 vs column 2). The integrin  $\alpha 3$  band was significantly enhanced by EtDO-P4 treatment (Fig. 6A, row 3; Fig. 6B-c, column 1 vs column 2). CD9 was reduced

by EtDO-P4 treatment (Fig. 6A, row 4; Fig. 6B-d, column 1 vs column 2). The degree of reduction for CD82 and CD81 bands by EtDO-P4 treatment was much greater (Fig. 6A, rows 5 and 6; Fig. 6B-e, -f, column 1 vs column 2). Reduced expression of these TSPs by EtDO-P4 treatment was clear in A431 cells, but expression

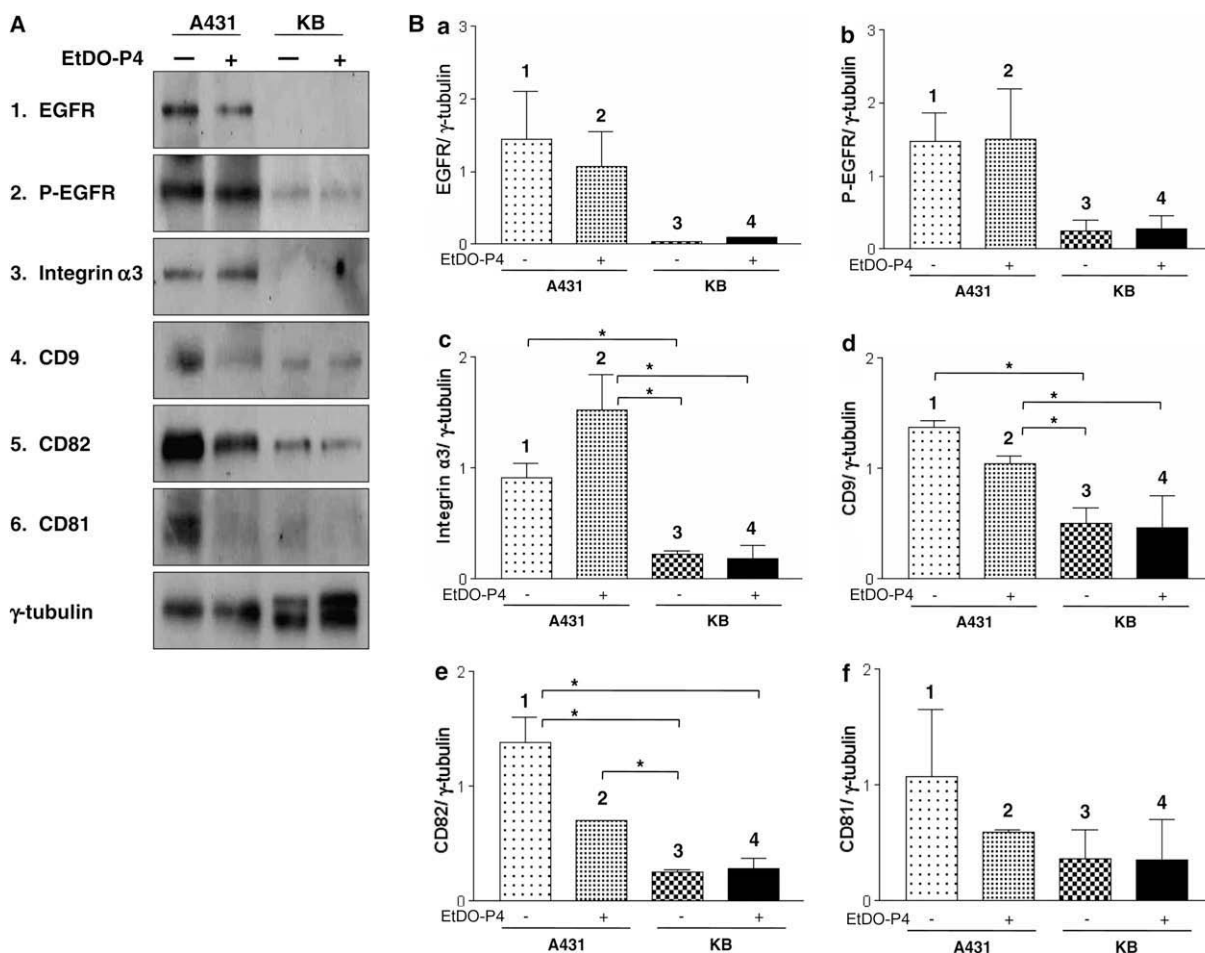


**Figure 6.** Effect of EtDO-P4 on expression of EGF, integrin  $\alpha 3$ , and tetraspanins in A431 and KB cells. A431 and KB cells ( $7 \times 10^5$ ) were cultured with or without  $1 \mu\text{M}$  EtDO-P4, followed by treatment of  $100 \text{ ng/mL}$  EGF as described in Section 2.7. Panel A: Cell lysate was subjected to Western blot analysis to determine expression of: 1, EGFR; 2, phosphorylated EGFR; 3, Integrin  $\alpha 3$ ; 4, CD9; 5, CD82; and 6, CD81, using respective antibodies. Band intensity was expressed relative to  $\gamma$ -tubulin as loading control, between EtDO-P4-treated A431 cells versus non-treated A431 cells. The same comparison was made for EtDO-P4-treated KB cells versus non-treated KB cells. Panel B: Effect of EtDO-P4 pre-treatment on band intensity of: a, EGFR; b, phosphorylated EGFR; c, Integrin  $\alpha 3$ ; d, CD9; e, CD82; and f, CD81. Height of columns 1, 2, 3, and 4 in each panel a–f is based on band intensity relative to  $\gamma$ -tubulin as the loading control, as in the ordinate. Standard deviation and significance of differences between columns, are shown. Significant differences ( $P < 0.01$ ) are indicated by an asterisk in parentheses ( ).

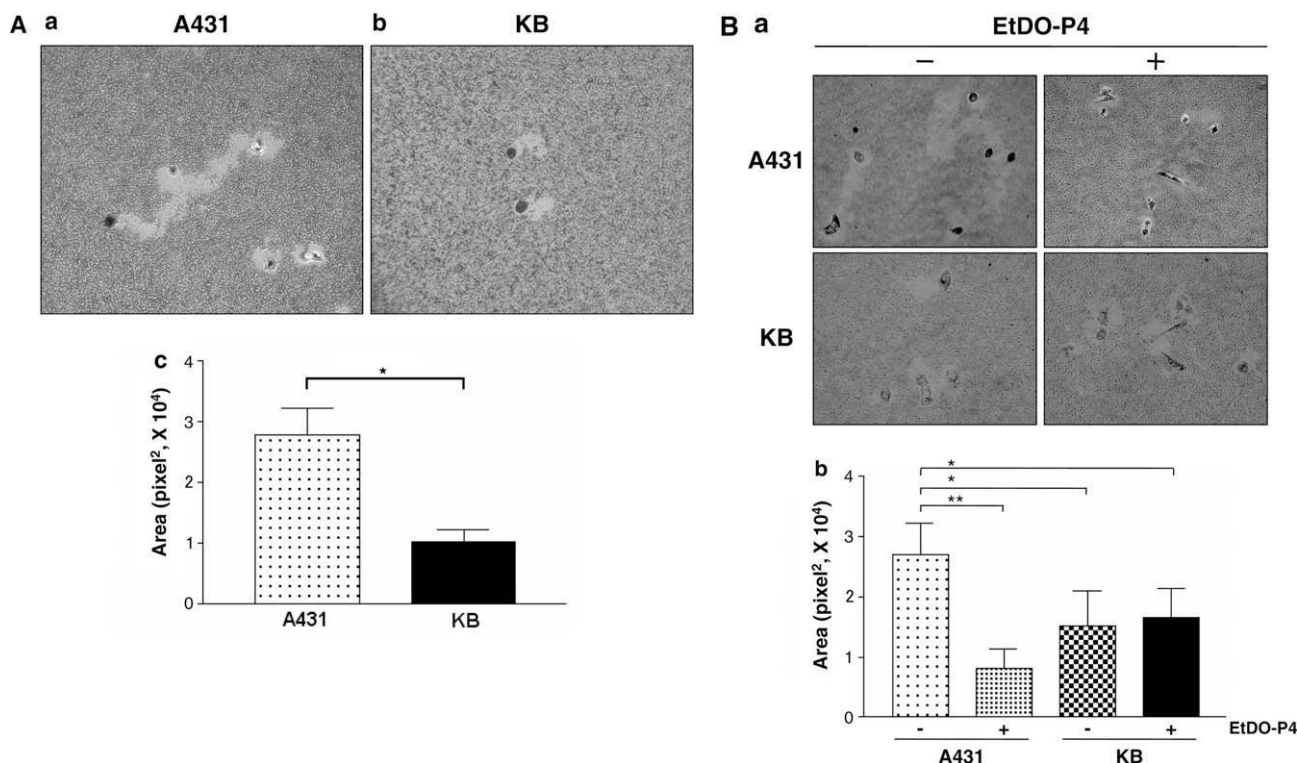


**Figure 7.** Cell motility determined by phagokinetic assay on a gold sol-coated plate. Panel A: Phagokinetic assay on gold sol-coated plate. A431 or KB cells ( $5 \times 10^2$ ) were cultured in a 24-well plate, and a phagokinetic assay was performed as described in Section 2.10. Examples of phagokinetic clearance of gold sol by A431 (a) and KB (b) cells. Panel c: motility difference between A431 and KB cells, based on cleared area of  $\geq 30$  cells, using the IMAGEJ program. Panel B: Effect of inhibition of GSL synthesis on cell motility. A431 and KB cells ( $5 \times 10^2$ ) were cultured with or without EtDO-P4, and phagokinetic assay was performed as described in Section 2.10. Experiments were repeated four times Standard deviation, and significance of differences between columns, are shown. \*,  $P < 0.005$ ; \*\*,  $P < 0.0001$ .

was low and unchanged in KB cells (Fig. 6A, rows 4, 5, and 6 under column KB; Fig. 6B-d, -e, and -f, columns 3 and 4). Similarly, levels of P-EGFR and integrin  $\alpha 3$  for KB were very low and unchanged by EtDO-P4 treatment (Fig. 6A, rows 2 and 3; Fig. 6B-b, and -c, columns 3 and 4).

### 3.7. Cell motility determined by the haptotactic method in A431 versus KB cells

Haptotactic motility determined on gold sol-coated plate, as described in Section 2.10, was much higher in A431 cells than in KB cells (Fig. 7A-a,b). Cleared area, determined by the IMAGEJ program, was significantly greater in A431 cells than in KB cells (Fig. 7A-c). In order to determine whether high motility of A431 cells is controlled by ganglioside GM2 and/or GM3, the effect of EtDO-P4 treatment on haptotactic cell motility was studied. The large the cleared area of KB cells was greatly reduced by EtDO-P4 treatment, whereas the cleared area of KB cells was unchanged (Fig. 7B-a). Quantitative motility difference in terms of squared pixels (ordinate) was compared in A431 and KB cells with EtDO-P4 treatment versus A431 and KB cells without EtDO-P4 treatment. The effect of EtDO-P4 is very clear in A431 cells, but not in KB cells (Fig. 7B-b).

### 3.8. Association of EGFR with TSP in A431 and KB cells

While levels of EGFR and TSPs CD9, CD81, and CD82 are much higher in A431 cells than in KB cells (see Figs. 1 and 6A and B), possible qualitative interaction between EGFR and TSP was studied by co-IP, based on the same quantity of protein solubilized in neutral detergent as described in Section 2.11. TSPs CD9, CD81, and CD82 were clearly co-IP'd with EGFR (Fig. 8). The level of TSP co-IP'd with EGFR was similar between A431 and KB cells.

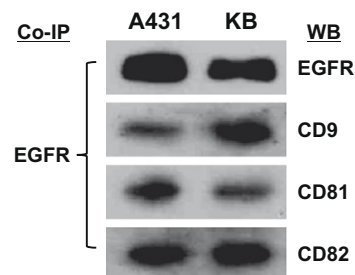


**Figure 8.** Association of EGFR with TSPs CD9, CD81, and CD82 in A431 versus KB cells. The post-nuclear fraction of cell lysate from A431 and KB cells was co-immunoprecipitated with anti-EGFR antibody as described in Section 2.11, and subjected to 12.5% SDS-PAGE and Western blot analysis using various anti-TSP antibodies.

## 4. Discussion

The growth-inhibitory effect rather than growth-inducing effect of EGF in A431 cells, particularly at high concentration (5–10 nM EGF), was described<sup>22–24</sup> soon after EGF, EGFR, and its associated kinases were discovered in the early 1980s.<sup>1–3</sup> This growth-inhibitory effect was correlated with unusually high expression of EGFR in A431 cells and its over-activated tyrosine kinase. While the exact mechanism is still unclear, it is assumed to be due in part to over-expenditure of intracellular ATP.<sup>25,26</sup>

While EGF-dependent growth properties of similar epidermoid carcinoma KB cells were studied previously to some extent,<sup>4</sup> the present study clearly established differential properties of KB versus A431 cells, in terms of expression of EGFR level, susceptibility to EGF, functional interaction of EGFR with TSPs, and ganglioside



interaction with TSPs. Among these, much higher motility of A431 cells than KB cells, based on much higher levels of both EGFR and TSPs in A431 cells than in KB cells, is a highly novel observation not found in previous studies. This is in striking contrast to the fact that EGFR tyrosine kinase activity is lower in A431 cells than in KB cells, particularly stimulated by EGF under serum-free conditions.

We previously demonstrated formation of complexes between gangliosides and TSPs, that is, GM3 with CD9,<sup>9,27</sup> GM3 with CD9–CD81,<sup>28,29</sup> and GM2 with CD82.<sup>10</sup> These complexes interact in turn with various growth factor receptors or integrin receptors, or affect functional interaction ('cross-talk') between growth factor receptors and  $\alpha 5$  or  $\alpha 3$  integrin.<sup>9–12,27–30</sup> In addition, a recent study indicates that the GM2–GM3 heterodimer conjugate, complexed with CD82, inhibits Met kinase.<sup>31</sup> However, all these ganglioside–TSP complexes inhibit, rather than promote, cell growth and motility. In striking contrast, results of the present study suggest a correlation between a high level of EGFR–TSP–GM3 or –GM2 complex and high motility in A431 cells. Motility is much lower in KB cells, possibly associated with low levels of EGFR and TSP in these cells.

EtDO-P4, the highly effective inhibitor of GlcCer synthase, which depletes all GSLs derived from GlcCer,<sup>15</sup> does not affect phosphorylation of EGFR in A431 or KB cells, indicating that GSLs, including GM2 and GM3, by themselves may not affect EGFR kinase activity. However, levels of CD82 and CD81 were significantly reduced by EtDO-P4 treatment, suggesting that these TSPs may be complexed with GM2 or GM3. As expected, A431 cell motility was significantly reduced by EtDO-P4 treatment (Fig. 7B), indicating that high A431 cell motility is maintained by gangliosides, organized with TSP and EGFR, possibly in glycosynaptic microdomain. Interaction of EGFR with all types of TSPs expressed in A431 cells was clearly indicated by co-IP data (Fig. 8).

Further detailed studies on TSP complexes with GM2 or GM3, or with GM2–GM3 heterodimer,<sup>31</sup> will help clarify their role in the functional interaction between growth factor receptors and integrins, to define tumor cell malignancy, which is based mainly on cell motility and invasiveness, rather than on simple cell growth.

## Acknowledgments

This study was supported by NIH Grant R01 CA80054 (to S.H.), and by a grant from the Korea Science and Engineering Foundation, and by the BK21 fellowship from the Department of Education, Republic of Korea (to S.P.). The authors thank James A. Shayman (Dept. of Internal Medicine, Univ. of Michigan) for a kind donation

of EtDO-P4, Reiji Kannagi (Aichi Cancer Center, Nagoya) for donation of anti-GM2 mAb MK1-8, and Steve Anderson for help with preparation of the manuscript and figures.

## References

- Ushiro, H.; Cohen, S. *J. Biol. Chem.* **1980**, *255*, 8363–8365.
- Cohen, S.; Carpenter, G.; King, L. *J. Biol. Chem.* **1980**, *255*, 4834–4842.
- Hunter, T.; Cooper, J. A. *Cell* **1981**, *24*, 741–752.
- Bremer, E. G.; Schlessinger, J.; Hakomori, S. *J. Biol. Chem.* **1986**, *261*, 2434–2440.
- Miljan, E. A.; Meuliet, E. J.; Mania-Farnell, B.; George, D.; Yamamoto, H.; Simon, H. G.; Bremer, E. G. *J. Biol. Chem.* **2002**, *277*, 10108–10113.
- Yoon, S.; Nakayama, K.; Hikita, T.; Handa, K.; Hakomori, S. *Proc. Natl. Acad. Sci. U.S.A.* **2006**, *103*, 18987–18991.
- Giard, D. J.; Aaronson, S. A.; Todaro, G. J.; Arnstein, P.; Kersey, J. H.; Dosik, H.; Parks, W. P. *J. Natl. Cancer Inst.* **1973**, *51*, 1417–1423.
- Eagle, H. *Proc. Soc. Exp. Biol. Med.* **1955**, *89*, 362–364.
- Ono, M.; Handa, K.; Sonnino, S.; Withers, D. A.; Nagai, H.; Hakomori, S. *Biochemistry* **2001**, *40*, 6414–6421.
- Todeschini, A. R.; Dos Santos, J. N.; Handa, K.; Hakomori, S. *J. Biol. Chem.* **2007**, *282*, 8123–8133.
- Mitsuzuka, K.; Handa, K.; Satoh, M.; Arai, Y.; Hakomori, S. *J. Biol. Chem.* **2005**, *280*, 35545–35553.
- Kawakami, Y.; Kawakami, K.; Steelant, W. F. A.; Ono, M.; Baek, R. C.; Handa, K.; Withers, D. A.; Hakomori, S. *J. Biol. Chem.* **2002**, *277*, 34349–34358.
- Miyake, M.; Ito, M.; Hitomi, S.; Ikeda, S.; Taki, T.; Kurata, M.; Hino, A.; Miyake, N.; Kannagi, R. *Cancer Res.* **1988**, *48*, 6154–6160.
- Dohi, T.; Nores, G.; Hakomori, S. *Cancer Res.* **1988**, *48*, 5680–5685.
- Lee, L.; Abe, A.; Shayman, J. A. *J. Biol. Chem.* **1999**, *274*, 14662–14669.
- Shu, L.; Lee, L.; Shayman, J. A. *J. Biol. Chem.* **2002**, *277*, 18447–18453.
- Kannagi, R.; Nudelman, E. D.; Levery, S. B.; Hakomori, S. *J. Biol. Chem.* **1982**, *257*, 14865–14874.
- Nakamura, K.; Suzuki, M.; Taya, C.; Inagaki, F.; Yamakawa, T.; Suzuki, A. *J. Biochem. (Tokyo)* **1991**, *110*, 832–841.
- Skipiski, V. P. *Methods Enzymol.* **1975**, *35*, 396–425.
- Ito, A.; Levery, S. B.; Saito, S.; Satoh, M.; Hakomori, S. *J. Biol. Chem.* **2001**, *276*, 16695–16703.
- Scott, W. N.; McCool, K.; Nelson, J. *Anal. Biochem.* **2000**, *287*, 343–344.
- Gill, G. N.; Lazar, C. S. *Nature* **1981**, *293*, 305–307.
- MacLeod, C. L.; Luk, A.; Castagnola, J.; Cronin, M.; Mendelsohn, J. *J. Cell. Physiol.* **1986**, *127*, 175–182.
- Barnes, D. W. *J. Cell Biol.* **1982**, *93*, 1–4.
- Gill, G. N.; Kawamoto, T.; Cochet, C.; Le, A.; Sato, J. D.; Masui, H.; McLeod, C.; Mendelsohn, J. *J. Biol. Chem.* **1984**, *259*, 7755–7760.
- Hanai, N.; Nores, G. A.; MacLeod, C.; Torres-Mendez, C.-R.; Hakomori, S. *J. Biol. Chem.* **1988**, *263*, 10915–10921.
- Ono, M.; Handa, K.; Withers, D. A.; Hakomori, S. *Cancer Res.* **1999**, *59*, 2335–2339.
- Toledo, M. S.; Suzuki, E.; Handa, K.; Hakomori, S. *J. Biol. Chem.* **2004**, *279*, 34655–34664.
- Toledo, M. S.; Suzuki, E.; Handa, K.; Hakomori, S. *J. Biol. Chem.* **2005**, *280*, 16227–16234.
- Satoh, M.; Ito, A.; Nojiri, H.; Handa, K.; Numahata, K.; Ohyama, C.; Saito, S.; Hoshi, S.; Hakomori, S. *Int. J. Oncol.* **2001**, *19*, 723–731.
- Todeschini, A. R.; Dos Santos, J. N.; Handa, K.; Hakomori, S. *Proc. Natl. Acad. Sci. U.S.A.* **2008**, *105*, 1925–1930.